Molecular Cell, Vol. 8, 1375–1382, December, 2001, Copyright ©2001 by Cell Press

Bacterial Polypeptide Release Factor RF2 Is Structurally Distinct from Eukaryotic eRF1

Bente Vestergaard,[1] Lan Bich Van,[1] Gregers R. Andersen,[1] Jens Nyborg,[1] Richard H. Buckingham,[2] and Morten Kjeldgaard[1,3]
[1] Institute of Molecular and Structural Biology
University of Aarhus
DK-8000 Aarhus C
Denmark
[2] Institut de Biologie Physico-Chimique
Centre National de la Recherche Scientifique
Unité Propre de Recherche 9073
Paris 75005
France

Summary

Bacterial release factor RF2 promotes termination of protein synthesis, specifically recognizing stop codons UAA or UGA. The crystal structure of *Escherichia coli* RF2 has been determined to a resolution of 1.8 Å. RF2 is structurally distinct from its eukaryotic counterpart eRF1. The tripeptide SPF motif, thought to confer RF2 stop codon specificity, and the universally conserved GGQ motif, proposed to be involved with the peptidyl transferase center, are exposed in loops only 23 Å apart, and the structure suggests that stop signal recognition is more complex than generally believed.

Introduction

In most bacteria, three codons are used as stop signals to trigger the hydrolysis of the ester bond between the tRNA bound in the ribosomal donor site (P site) and the polypeptide chain, leading to its release. The presence of a stop codon in the A site is sensed by release factors (RF) that interact with the ribosome and promote peptidyl-tRNA hydrolysis (for a recent review, see Kisselev and Buckingham, 2000). RFs are grouped into two subclasses. The class II RF3 stimulates termination by the recycling of class I RFs in a GTP-dependent manner but do not contribute to termination nor to the catalysis of peptide chain release (Freistroffer et al., 1997). Class I RFs enter the ribosomal A site and promote hydrolysis of the ester bond in response to specific codons. In eukaryotes and archaea, the three stop codons are recognized by one omnipotent class I RF, termed eRF1 and aRF1, respectively. In bacteria, two class I RFs, which share high sequence similarity, show semispecific stop codon recognition in that both factors recognize stop codon UAA, whereas UAG and UGA are specifically recognized by RF1 and RF2, respectively. Class I RFs are functionally comparable to a tRNA molecule in that RFs bind to the ribosomal A site in a sequence-specific manner. Class I RFs have been proposed to be an example of macromolecular mimicry (Ito et al., 1996), as was first discovered through comparison of the crystal structure of EF-G:GDP (Czworkowski et al., 1994) and that of the ternary complex EF-Tu:GTP:aa-tRNA (Nissen et al., 1995). Subsequently the crystal structure of RRF (Selmer et al., 1999) has provided another example of tRNA mimicry. The structure of human eRF1 (Song et al., 2000) also shows features of the typical tRNA L shape, although the resemblance is much less striking. There is no overall sequence homology between bacterial class I RFs and their eukaryotic/archaeal counterparts (Kisselev et al., 2000; Song et al., 2000); only a short motif is universally conserved, comprising the tripeptide GlyGlyGln (GGQ) (Frolova et al., 1999). Mutations to either of the conserved glycine residues in human eRF1 do not affect ribosome binding but abolish release activity, and it has been proposed that the motif participates directly in peptide hydrolysis (Frolova et al., 1999). However, mutation of the Gln residue only partly destroys release activity in vitro (Seit Nebi et al., 2000), refuting the suggestion that the residue coordinates a water molecule in the ribosomal peptidyltransferase center (PTC) (Song et al., 2000).

Residue 246 in *E. coli* RF2 is a threonine in strain K12, whereas it is a conserved alanine or serine in other known bacterial sequences of RF2, including other strains of *E. coli* (Dincbas-Renqvist et al., 2000). *E. coli* K12 RF2 is toxic when overexpressed, but cell viability is restored by the single mutation Thr246Ala (Uno et al., 1996) or Thr246Ser (Wilson et al., 2000). Thr246 is in close proximity to residues GGQ250–252, and the conserved glutamine is posttranslationally N-methylated. It has been shown that the toxicity arises from the accumulated effects of lack of methylation of Gln252 and of having a threonine at position 246 (Dincbas-Renqvist et al., 2000).

A tripeptide motif in bacterial class I RFs, ProXxxThr and SerProPhe (SPF) in RF1 and RF2, respectively (Ito et al., 2000), confers stop codon specificity in a hybrid RF1/RF2 protein. These tripeptides have been hypothesized to interact directly with the second and third codon nucleotide (Ito et al., 2000). The question as to whether RFs interact directly or indirectly with the stop codon is one of long standing. The hypothesis of direct interaction has been supported by the formation of crosslinks between stop codons and both RF2 (Poole et al., 1998) and eRF1 (Chavatte et al., 2001). However, the precise regions of the RFs involved have not yet been identified. An alternative viewpoint emphasizes the role that may be played by interactions between the stop signal and defined nucleotides in 16S and 30S rRNA based on the effects of mutations affecting these molecules (Arkov and Murgola, 1999).

Results

Structure Determination

Crystals of *E. coli* K12 Thr246Ala RF2 were obtained using the method of vapor diffusion. The crystals grew in flower-like bundles, each leaf of a size of approximately $250 \times 150 \times 10\ \mu m^3$.

Data were collected using synchrotron radiation at the Ellettra Synchrotron Light Source, Trieste, Italy. RF2

[3] Correspondence: mok@imsb.au.dk

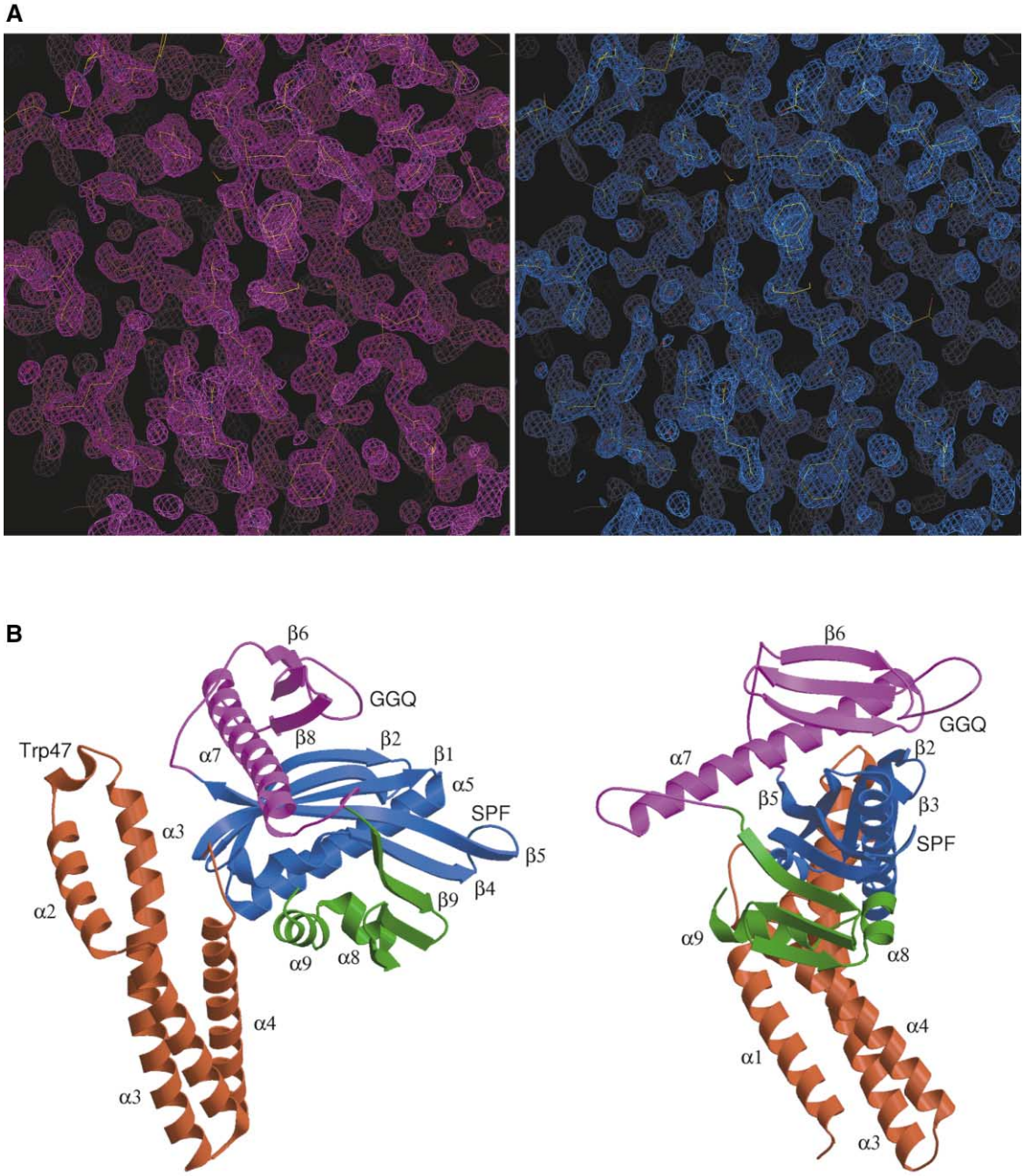

Figure 1. Structural Presentation of *E. coli* RF2

(A) Electron density, contoured at 1.8σ, showing the central β sheet of domain 2. Experimental map calculated from data from crystal #2 (left) and final $3F_o - 2F_c\ \sigma_A$ weighted map (right). The refined model of *E. coli* RF2 is shown in sticks.

(B) Cartoon presentation of *E. coli* RF2. On the right, the molecule is rotated 90° around the vertical axis with respect to the orientation on the left. The functionally important SPF and GGQ motifs are exposed on the curved surface of the molecule. Domain 1 is shown in orange, domain 2 is in blue, domain 3 is in magenta, and domain 4 is in green. The figure was prepared using MolScript and Raster3D.

crystallizes in spacegroup $P2_1$ with cell parameters a = 57.38 Å, b = 49.89 Å, c = 63.14 Å, β = 107.0°. The crystal structure of RF2 was determined using the single wavelength anomalous dispersion technique (SAD). The data extends to 1.8 Å, and the experimental map is of very high quality (Figure 1A). The GGQ loop is poorly resolved in the electron density, indicating that it is mobile and thus disordered in the crystals. Hence, residues 247–257 were modeled mainly based on crystal packing. Another loop (residues 310–319) has high B factors but is clearly visible in the electron density. The final model comprises residues 4–365 and includes 286 ordered water molecules. The model was refined using CNS (Brünger et al., 1998) to a final R/R_{free} of 22.2%/24.7% using all data in the range between 50 Å and 1.8 Å (see Table 1).

Table 1. Refinement Statistics on Crystal #2	
Resolution range (Å)	50–1.8
Reflections, total	59,537
Reflections, validation set	2,957 (4.8%)
Protein atoms	2,866
Water molecules	286
R value	0.222 (0.278)
R_{free}	0.247 (0.310)
Deviation from Ideality (rmsd)	
Bond lengths (Å)	0.005
Bond angles (°)	1.12
Improper angles (°)	0.687
Dihedral angles (°)	21.25
Minimum/maximum B factor (Å^2)	7.35/116.92
Average B factor (Å^2)	27.53
Ramachandran Plot[a]	
In favorable region	92.8%
Additionally allowed	6.6%
Generously allowed	0.6%
Disallowed[b]	0%

Numbers in parentheses give the value of the highest resolution shell of the data, unless otherwise stated.
[a] Nonglycines, nonprolines.
[b] Residues in regions of weak electron density.

E. coli RF2 is composed of four domains (Figure 1B). The N-terminal domain 1 (residues 1–116, orange in Figure 1B) consists of four α helices and a short 3_{10} helix. Helix α3 (51–90) spans the entire length of the domain. Helices α1, α3, and α4 form a classical three-stranded coiled coil, and helices α2 and α3 form a two-stranded coiled coil. The two-stranded coiled coil bends away from the bulk structure but is anchored to the rest of the structure by polar interactions. The three-stranded coiled coil of domain 1 is a fold also known from RRF (Protein Data Bank accession number 1dd5). In RRF this domain is proposed to mimic the anticodon stem of tRNA (Selmer et al., 1999).

A short spacer leads from domain 1 to domain 2 (125–225). Domain 2 (blue in Figure 1B) is composed of a five-stranded antiparallel β sheet and two α helices. The β sheet wraps around the long central helix α5 (residues 139–159). The SPF motif is situated in a loop between strands β4 and β5 at the end of the β sheet opposite to domain 1. The first turn of the shorter helix α6 is a 3_{10} helix. Domain 2 has structural homology to ribosomal proteins S6 and S10 (PDB accession numbers 1fjf and 1ris).

Above the β sheet of domain 2 is domain 3 (magenta in Figure 1B). Strands β6, β7, and β8 form a three-stranded antiparallel β sheet and a 45 Å long α helix protrudes from the bulk of the structure. This long helix forms the majority of the interface to domain 2. The first 13 residues of domain 3 (226–238) form an unusual loop that wraps halfway around the diameter of the helix. In another loop, the GGQ motif is distally situated in the domain. Domain 3 has structural homology to ribosomal proteins S5 (PDB accession numbers 1pkp and 1fjf) and S11 (1fjf).

The C-terminal domain (green in Figure 1B) packs against the central domain 2 by extending the β sheet with three further strands, thereby completing an eight-stranded open bowl. The first strand is parallel to the adjacent strand from domain 2, and the three strands of domain 4 are antiparallel. The domain ends with two short α helices that are tightly packed against domain 2 as well. Domains 2 and 4 are closely connected and in reality form a single domain. An extensive network of aromatic residues, many of which are highly conserved (Figure 2A), stabilizes the hydrophobic core of this superdomain. Furthermore, a cluster of conserved polar residues connected in a hydrogen bonded network is located in the center of the domain.

Overall, domains 2, 3, and 4 form a very compact structure held together by multiple polar and nonpolar interactions. Domain 1 protrudes from the main body of the domain but is anchored to the rest of the protein via a patch of hydrophobic residues and several salt bridges and hydrogen bonds. One side of the structure forms a large smoothly curved surface (Figure 1B), and the functionally important SPF and GGQ motifs are exposed in loops on this face.

Crystal Packing

Experimental electron density maps were computed from each data set on three different crystals. Each of the three crystals had different cell parameters (Table 2), most likely due to different cryo conditions used in the low-temperature data collection. The crystal consists of layers of molecules along the b and c directions of the unit cell. All domains are involved in forming the crystal contacts. In crystals 1 and 2, there has been a sliding of these layers mainly in the c direction, allowing the layers to pack 11 Å closer to each other along the a direction. The unique β angle changes by 10°. Thus, the crystal contacts are very different in the two crystal forms, and specifically a close contact between the tip of the three-stranded coiled coil and helix α8 of domain 4 changes significantly. Yet, the conformation of the RF2 molecule is unchanged. Therefore, from these observations there is no evidence of interdomain flexibility.

Conserved Residues

Looking at the smoothly curved surface of the molecule (bottom, Figure 2A), the exposed conserved residues Arg150, Asp350, and Arg154 form a network between domains 2 and 4. Furthermore, areas surrounding the loops containing the GGQ and SPF-motifs are conserved, as are residues Trp47, Glu157, and Arg278. These and a few conserved acidic residues in domain 1 are not important for maintaining the tertiary structure.

On the other side of the molecule (top, Figure 2A), only a few conserved residues are visible on the surface. In domain 1, Glu85 is highly conserved. The completely conserved aromatic residue Tyr296 is also visible. It forms part of a conserved aromatic network in the core formed by residues Tyr189, Pro224 (domain 2), and Tyr296 (domain 3). The network is further extended to domain 1 via residues Tyr187 and Trp191 on the short helix α6 in domain 2 interacting with residues Phe161 (domain 2), Tyr123, and Tyr115 (domain 1). The conserved Arg337 is also exposed on the surface. It forms a hydrogen bond to the backbone oxygen of residue 194 in domain 2. Apart from those structurally conserved residues, a patch across the β sheet of domains 2 and 3 is conserved.

A

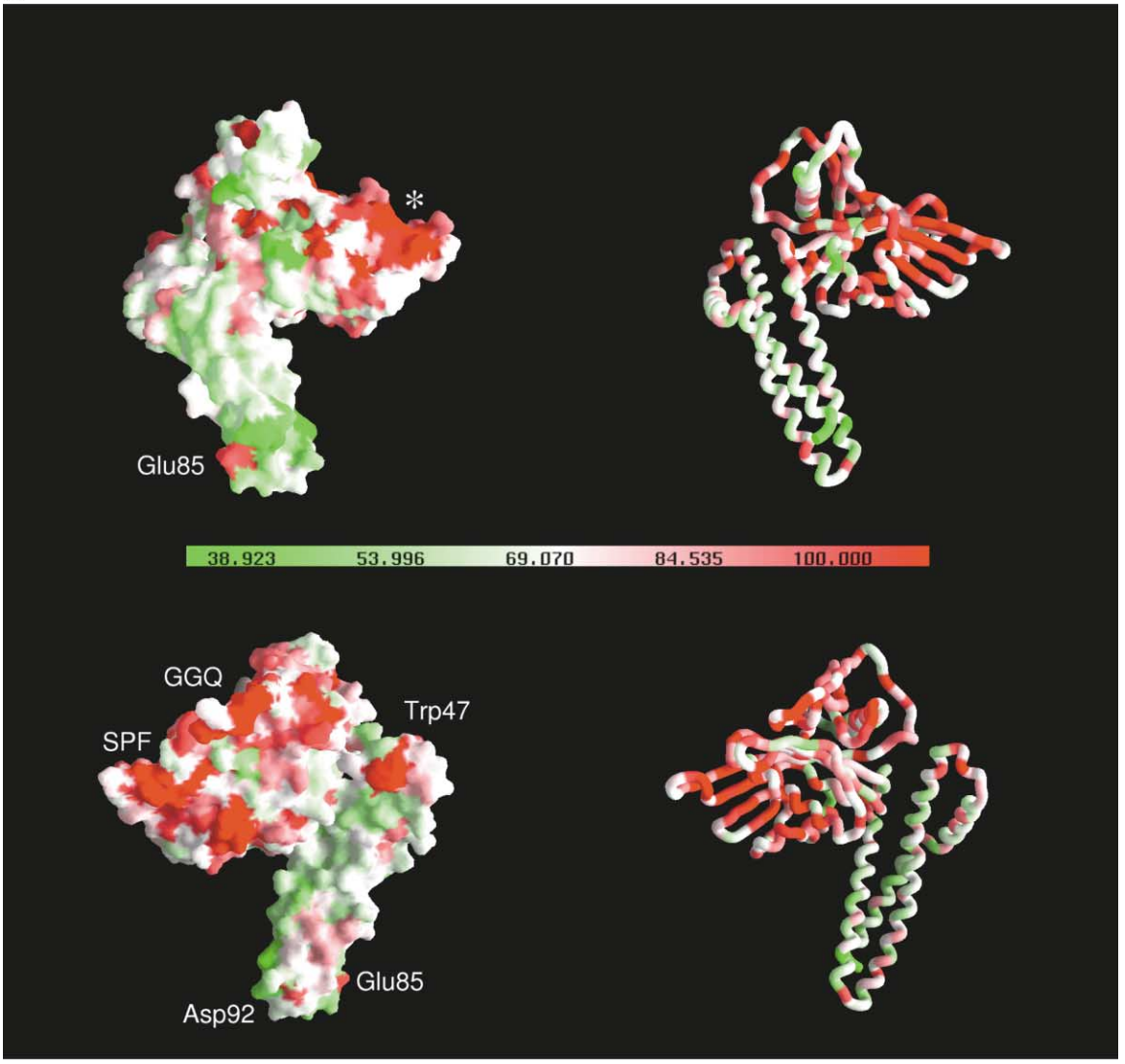
*
Glu85
38.923
53.996
69.070
84.535
100.000
GGQ
Trp47
SPF
Glu85
Asp92

B

```
                                                
```

Table 2. Crystallographic Statistics

Crystal Number	1	2	3
High resolution limit (Å)	2.2	1.8	2.5
Degrees of data	240	240	450
Reflections recorded (unique)[a]	319,063 (34,434)	1,018,104 (58,787)	371,410 (29,058)
Cell parameters (Å)	a = 58.372, b = 50.346, c = 63.659, β = 107.54°	a = 57.388, b = 49.893, c = 63.144, β = 107.01°	a = 68.147, b = 50.138, c = 64.076, β = 117.26°
Crystal mosaicity	1.0°	1.5°	1.0°
R_{merge} overall	0.052 (0.200)	0.070 (0.319)	0.082 (0.378)
Completeness	99.6% (99.7%)	95.9% (71.2%)	99.9% (100.0%)
Average redundancy	2.5	2.3	4.9
Average I/σ(I)	16.0 (3.2)	12.3 (1.7)	18.2 (3.3)
Cullis R value	0.7078 (0.7808)	0.6922 (0.7870)	0.7486 (0.9067)
Kraut R value	0.0506 (0.1281)	0.0454 (0.1524)	0.0390 (0.0933)
Phasing power	1.1081 (0.4609)	1.1816 (0.5471)	0.9545 (0.2355)
Figure of merit	0.2549 (0.0949)	0.2731 (0.1661)	0.2103 (0.0389)
Cryo protection	10% glycerol	10% sucrose	10% ethylen glycol
Phased using sepositions from	Model	Model	Anomalous Patterson

Statistics on the three data sets. Numbers in parentheses give the value of the highest resolution shell of the data, unless otherwise stated.
[a] Bijvoet pairs kept separately.

The present crystal structure of *E. coli* RF2 shows that domain 1 points away from the main body of the structure. A computer-generated sequence alignment of domain 1 of bacterial RF1 and RF2 reveals a low degree of conservation. However, the present structure of *E. coli* RF2 makes it possible to identify structurally conserved residues in this domain that are also conserved in RF1 (Figure 2B). Lys58 (*E. coli* RF2 numbering) is situated in helix α3 and forms a salt bridge across the crevice between domains 1 and 2 to Asp127. The conserved Glu59 on helix α3 forms a salt bridge to Arg33 in helix α2 and stabilizes the two-stranded coiled coil. Asp124 in the linker between domains 1 and 2 forms a salt bridge to Arg193 in domain 2. The completely conserved glycines 137 and 138 form a tight loop from strand β1 to helix α5.

The amino acid residues between the structurally conserved residues comprise the helix-loop-helix motif from the tip of domain 1. This intervening sequence cannot be aligned between RF1 and RF2 as the two factors each have their own conserved motifs.

Only a few of the conserved residues in this area are conserved for structural reasons. RF1 has a completely conserved proline at a position corresponding to Tyr123 in *E. coli* RF2. In RF2, this residue is part of a large hydrophobic network. In RF2, Asp114 in helix α4 interacts with Arg17 in helix α1, thereby stabilizing the three-stranded coiled coil. There is no counterpart in RF1, as the RF1 sequence is shorter than RF2 at the N terminus.

The conserved acidic residues 79, 85, 92, and 102 of RF2 are not part of any intramolecular contacts and must be conserved for other reasons. In RF1, three acidic residues are highly conserved. According to secondary structure predictions and the alignment presented, helix α3 and α4 of RF1 will, respectively, be approximately one turn shorter and one turn longer than the corresponding helices in RF2 (Figure 2B). This will inevitably position the conserved acidic residues at the tip of domain 1 differently in RF1 and RF2.

Comparison with Human eRF1

The tertiary structure of human eRF1 (Song et al., 2000) shares no similarity to that of *E. coli* RF2. Human eRF1 adopts a Y-like shape in a three-domain structure, and there are few interdomain contacts. None of the three domains resembles any domain in RF2. The GGQ motif is exposed in a loop at the tip of domain II in eRF1. A conserved motif, NIKS, thought to mimic the anticodon of tRNA, lies in domain I. The NIKS and GGQ motifs are 99.5 Å apart, measured as the distance between the Cα positions of the two closest residues (Asn61 and Gln185) and not 80 Å as stated in the original paper (Song et al., 2000). The authors offer no explanation for the problems with fitting a molecule this size into the ribosomal A site. Most likely, eRF1 changes conformation upon binding to eRF3. In *E. coli* RF2, the proposed anticodon-mimicking tripeptide SPF (Ito et al., 2000) is only 23 Å away from the GGQ motif. Thus, it is obvious that the SPF loop and the GGQ loop of *E. coli* RF2 do not correspond to the proposed anticodon mimic and GGQ loop of eRF1. Despite their functional similarity, human eRF1 and *E. coli*

Figure 2. Conserved residues in *E. coli* RF2

(A) Surface (left) and snake (right) presentation of *E. coli* RF2. Residues are colored according to the degree of conservation among bacterial RF2, ranging from green (low) to red (high). The asterisk marks a conserved area across the β sheet of domains 2 and 4. Trp47, the SPF motif, and the GGQ motif are marked. The surface representation was made using GRASP and color-coded according to a sequence alignment produced by the ClustalW program.

(B) Alignment of *E. coli* RF2 residues 56–138 in domain 1 with bacterial RF2 (top) and RF1 (bottom). Above the observed secondary structure of RF2 and a computer-generated predicted secondary structure of RF1 is depicted. "H" signifies α helix, "E" indicates β strand, and "C" indicates coil. Residue numbers above the conserved motifs correspond to *E. coli* RF2 numbering. Below, a bar marks the borders of structurally conserved and structurally distinct areas, respectively.

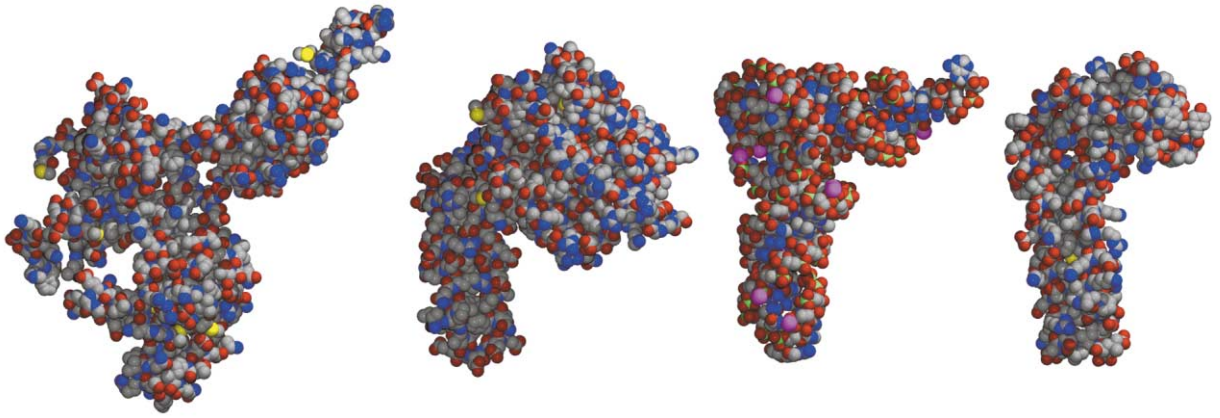

Figure 3. Macromolecular Mimicry in Termination and Ribosome Recycling

CPK representations of (left to right) human eRF1, *E. coli* RF2, yeast $tRNA^{Phe}$, and *Thermotoga maritima* RRF. The orientation of eRF1 relative to tRNA is similar to what is proposed by Song et al. (2000), and the orientation of RRF relative to tRNA was proposed by Selmer et al. (1999).

RF2 are completely distinct proteins in terms of primary, secondary, and tertiary structure (Figure 3).

Discussion

Is RF2 a tRNA Mimic?

As both class I RFs and RRF are suggested to be examples of macromolecular mimicry, the structure of RF2 was superimposed onto the structure of $tRNA^{Phe}$ (Jovine et al., 2000). The distance between SPF205–207 and GGQ250–252 is only 23 Å; thus, it is immediately obvious that these two motifs of *E. coli* RF2 cannot span the distance from the ribosomal decoding site to the PTC (Figure 1B). Therefore, the previously obtained biochemical results do not offer a clear answer as to how RF2 should be oriented.

In order to investigate the suggestion that SPF is the anticodon-mimicking tripeptide (Ito et al., 2000), domain 2 with the SPF motif was superimposed on the anticodon of a tRNA molecule, and the general overlay of the two structures was visually optimized. In this orientation, RF2 was then docked onto the A site of the 5.5 Å model of the *Thermus thermophilus* 70S ribosome (Yusupov et al., 2001), but the model was rejected since RF2 seriously clashes with rRNA.

The GGQ motif has been suggested to be in close contact with the peptidyl transferase center (PTC) of the ribosome (Frolova et al., 1999). Placing the GGQ loop toward the CCA end of the tRNA, RF2 can be oriented such that domain 1 superimposes on the anticodon stem loop (ASL) and domains 2, 3, and 4 cover the acceptor arm of tRNA (Figure 3). In this orientation, the molecule could be placed in a tight fit in the ribosomal A site, avoiding any spatial clashes with the ribosome and at the same time placing all conserved areas on the surface of RF2 in contact with rRNA. An exception is the conserved patch on the face of the β sheet of domains 2 and 4 (Figure 2A, top) that is oriented toward the factor binding site and thus could be important for interaction with RF3. The curved surface of *E. coli* RF2 (Figure 1B, right) forms the majority of the contact area between RF2 and the ribosome. In this model for the binding of RF2 to the ribosomal A site, RF2 spans the distance from the 30S decoding center to the 50S PTC by contact between conserved motifs and rRNA, with the universally conserved GGQ loop contacting the A loop of the PTC. The GGQ loop protrudes from a domain with structural homology to ribosomal protein S5. The crystal structure of S5 has been determined both for the isolated protein and on the 30S subunit (PDB entry 1pkp and 1fjf). On the ribosome, the loop of S5 that corresponds to the GGQ loop in domain 3 changes to a straight β hairpin, which is not found for the isolated protein. This loop is inserted between rRNA loops and contains a conserved GGR motif, which is exposed at the tip of the β hairpin where the arginine interacts with rRNA. If the GGQ loop of domain 3 adopts a similar conformation on the ribosome, the GGQ motif reaches further into the PTC. If the GGQ loop of RF2 only adopts such a fixed conformation on the ribosome, this would explain the disordering of the loop in the present study.

In this model the functionally important tripeptide SPF docks onto the 16S rRNA helix 44 that has been shown to be of major importance for intersubunit signaling on the ribosome during the various states of translation (Carter et al., 2000).

Conclusion

The crystal structure of release factor RF2 Thr246Ala from *E. coli* K12 has been determined to 1.8 Å resolution using the SAD-phasing method. The structure is composed of four domains, and biochemically important residues are exposed in loops on the surface of the molecule. The primary, secondary, and tertiary structure of *E. coli* RF2 is different from that of eRF1 although the two factors are functionally similar. The RF2-specific tripeptide SPF motif, earlier proposed to be a "peptide anticodon," and the universally conserved GGQ motif are at an approximate distance of 23 Å from each other. It is therefore concluded that the formerly existing dogmas that SPF directly interacts with the stop codon and that GGQ contacts the PTC cannot both be true at the same time. The GGQ loop is highly flexible and may assume an extended hairpin conformation upon binding

to the ribosome similar to what has been observed for the ribosomal protein S5. Such a change, however, will not be large enough to solve the conflict between existing dogmas.

A hypothetical model for binding of RF2 to the ribosome, based on the concept of macromolecular mimicry (Nissen et al., 1995) and three-dimensional fit with the 70S ribosome (Yusupov et al., 2001), is presented, and RF2 spans the distance from the decoding site of the small subunit to the PTC of the large subunit via conserved residues including the SPF and GGQ motifs. RF2 thus links the presence of a stop codon on mRNA to hydrolysis of the peptidyl-tRNA ester bond. The perception of RF2 being merely a tRNA mimic that spans from the anticodon loop to the CCA end thus is too simple, and RF2 most likely achieves its role of triggering peptidyl-tRNA hydrolysis only by functioning in close concert with rRNA. In the light of the new structural information, further biochemical experiments need to be performed to obtain insight into semispecific stop codon interaction and release function.

Experimental Procedures

Cloning, Expression, and Purification

The clone of *E. coli* K12 RF2 Thr246Ala mutant (Dincbas-Renquist et al., 2000) was overexpressed in *E. coli* cells strain B834(DE3) (Novagen). Selenomethionine was incorporated in a minimal medium containing 40 mg/l of all amino acids except methionine and an additional 40 mg/l of selenomethionine. The medium contained 1 mg/l vitamins (riboflavin, niacinamide, pyridoxine monohydrochloride, and thiamine), 25 mg/l $FeSO_4$, 0.4% glucose, 2 mM $MgSO_4$, 2 g/l NH_4Cl, 6 g/l KH_2PO_4, and 25.6 g/l $Na_2HPO_4 \bullet 7H_2O$. Kanamycin (50 mg/l) and ampicillin (100 mg/l) were added. The cells grew to an OD_{600} of approximately 0.6 before inducing with 0.5 mM final concentration of isopropyl-1-thio-D-galactoside (IPTG). Expression continued for 7 hr. Harvested cells were opened in 30 mM TrisHCl, 150 mM NaCl, 10% glycerol, 10 mM DTT, 100 μM PMSF, 10 mg/l DNAase I, using a French pressure cell. The opened cells were centrifuged at 40,000 rpm for 1h, and the filtered supernatant was loaded onto a Q sepharose FF (Pharmacia) column equilibrated in the above-mentioned buffer. A linear gradient from 150 mM NaCl to 1 M NaCl eluted the protein. $(NH_4)2SO_4$ (AmS) was added to the pool containing RF2 to a final concentration of 1.6 M, and the protein was left at 0°C for 1h before filtrating and loading to a Phenyl-Sepharose FF (Pharmacia) column, equilibrated in buffer A (30 mM MES [pH 6.0], 50 mM NaCl, 10% glycerol, 5 mM DTT) with an addition of 2.0 M AmS. After extensive washing with buffer A, RF2 was step eluted from the column using 50 mM CHES (pH 9.0), 50 mM NaCl, 10% glycerol, 5 mM DTT. Finally, the protein was loaded onto a Source-Q column (Pharmacia) equilibrated in buffer A. A gradient from 100% A to 100% B (30 mM TrisHCl [pH 8.0], 500 mM NaCl, 10% glycerol, 5 mM DTT) eluted the protein at approximately 70% B. Fractions from the last purification step were kept separate.

Crystallization

Crystallization was carried out at 20°C using the method of vapor diffusion. Crystallization of the protein was highly dependent on nucleation, and reproduction of crystals was difficult. The reservoir contained 40 mM TrisHCl (pH 7.6), 400 mM NaCl, 40 mM $MgCl_2$, 2% ethylene glycol, 20 mM DTT, and PEG 2k MME from 28%–34%. The protein concentration was between 3.5 mg/ml and 8.0 mg/ml in the reservoir buffer without PEG 2k MME. The protein was kept at 0°C for 1h after the addition of PEG2k MME to 15%, filtered (0.2 μm syringe filters), and centrifuged at 12,000 rpm for 20 min immediately prior to mixing the drops. Crystals grew within 2 days and were left to increase in size for 2 weeks prior to cryo protection and data collection (Table 2).

Data Collection and Structure Determination

The data were collected at the Elettra Synchrotron Light Source, Italy, using a MAR CCD area detector. Three independent data sets were collected (Table 2). A flourescence spectrum was measured, and the wavelength was set at the absorption peak, close to theoretical value from the selenium K edge (0.9795 Å). The monochromator of the beamline was adjusted to give higher intensity at the expense of energy discrimination, and the $\Delta\lambda$ of the transmitted beam was 3 eV where 1 eV is normally required for a MAD experiment. On two crystals 240° of data and on the third 450° of data were collected. All crystals were anisotropic and exhibited high mosaic spread. The data were reduced and scaled using the HKL program suite using the SCALE ANOMALOUS mode in SCALEPACK. The anomalous Patterson Harker sections clearly showed seven peaks. Location of the positions of the anomalous scatterers and the SAD phasing were carried out using slightly modified scripts for the CNS package (Brünger et al., 1998). The model was built using the O program (Jones and Kjeldgaard, 1997), first using the data set of crystal #3. Refinement was carried out using the simulated annealing protocol of CNS. Five percent of the reflections were used for validation. The model built from the data set of crystal #3 was subsequently used to build a model in preliminary experimental electron density maps derived from the data sets from crystals #1 and #2. This initial model was used to redetermine the Se positions, and a new experimental SAD phasing was carried out on each data set. In the protein structure refinement, the maximum-likelihood Hendrickson-Lattman (MLHL) target was used, which uses the experimentally available phase information to guide the refinement.

Acknowledgments

We thank Jane MacDougall for starting the project with much enthusiasm. We are grateful to Massimo Degano, Alberto Cassetta, and Doriano Lamba at Elettra for their support with the data collection. We thank Poul Nissen for enthusiasm and inspiring discussions, Ray Brown for continuing advice on laboratory work and procedures, and Ditlev Brodersen and Venki Ramakrishnan for relevant suggestions and comments on the manuscript. M.K. is a recipient of the Hallas-Møller fellowship from the Novo-Nordisk Foundation. B.V. has received a PhD fellowship from and the work in general was supported by the EU-project on *Inhibition of Transitions in Protein Synthesis: Protein-Structure Approach to Antibiotic Development* (Contract no BIO4-97-2188), and R.H.B. is supported by the Centre National de la Recherche Scientifique (UPR9073).

Received August 20, 2001; revised November 7, 2001.

References

Arkov, A.L., and Murgola, E.J. (1999). Ribosomal RNAs in translation termination: facts and hypotheses. Biochemistry *64*, 1354–1359.

Brünger, A.T., Adams, P.D., Clore, G.M., DeLano, W.L., Gros, P., Grosse-Kunstleve, R.W., Jiang, J.S., Kuszewski, J., Nilges, M., Pannu, N.S., et al. (1998). Crystallography & NMR system: a new software suite for macromolecular structure determination. Acta Crystallogr. D Biol. Crystallogr. *54*, 905–921.

Carter, A.P., Clemons, W.M., Brodersen, D.E., Morgan-Warren, R.J., Wimberly, B.T., and Ramakrishnan, V. (2000). Functional insights from the structure of the 30S ribosomal subunit and its interactions with antibiotics. Nature *407*, 340–348.

Chavatte, L., Frolova, L., Kisselev, L., and Favre, A. (2001). The polypeptide chain release factor eRF1 specifically contacts the s(4)UGA stop codon located in the A site of eukaryotic ribosomes. Eur. J. Biochem. *268*, 2896–2904.

Czworkowski, J., Wang, J., Steitz, T.A., and Moore, P.B. (1994). The crystal structure of elongation factor G complexed with GDP, at 2.7 Å resolution. EMBO J. *13*, 3661–3668.

Dincbas-Renqvist, V., Engstrom, A., Mora, L., Heurgue-Hamard, V., Buckingham, R., and Ehrenberg, M. (2000). A post-translational modification in the GGQ motif of RF2 from Escherichia coli stimulates termination of translation. EMBO J. *19*, 6900–6907.

Freistroffer, D.V., Pavlov, M.Y., MacDougall, J., Buckingham, R.H.,

and Ehrenberg, M. (1997). Release factor RF3 in E.coli accelerates the dissociation of release factors RF1 and RF2 from the ribosome in a GTP-dependent manner. EMBO J. *16*, 4126–4133.

Frolova, L.Y., Tsivkovskii, R.Y., Sivolobova, G.F., Oparina, N.Y., Serpinsky, O.I., Blinov, V.M., Tatkov, S.I., and Kisselev, L.L. (1999). Mutations in the highly conserved GGQ motif of class 1 polypeptide release factors abolish ability of human eRF1 to trigger peptidyl-tRNA hydrolysis. RNA *5*, 1014–1020.

Ito, K., Ebihara, K., Uno, M., and Nakamura, Y. (1996). Conserved motifs in prokaryotic and eukaryotic polypeptide release factors: tRNA-protein mimicry hypothesis. Proc. Natl. Acad. Sci. USA *93*, 5443–5448.

Ito, K., Uno, M., and Nakamura, Y. (2000). A tripeptide 'anticodon' deciphers stop codons in messenger RNA. Nature *403*, 680–684.

Jones, T.A., and Kjeldgaard, M. (1997). Electron density map interpretation. In Methods in Enzymology, Volume 277, C.W. Carter, Jr. and R.M. Sweet, eds. (New York: Academic Press), pp. 173–208.

Jovine, L., Djordjevic, S., and Rhodes, D. (2000). The crystal structure of yeast phenylalanine tRNA at 2.0 Å resolution: cleavage by Mg(2+) in 15-year old crystals. J. Mol. Biol. *301*, 401–414.

Kisselev, L.L., and Buckingham, R.H. (2000). Translational termination comes of age. Trends Biochem. Sci. *25*, 561–566.

Kisselev, L.L., Oparina, N.Y., and Frolova, L. (2000). Class-1 polypeptide chain release factors are structurally and functionally similar to suppressor tRNAs and comprise different structural-functional families of prokaryotic/mitochondrial and eukaryotic/archaebacterial factors. Mol. Biol. (Mosk.) *34*, 363–442.

Nissen, P., Kjeldgaard, M., Thirup, S., Polekhina, G., Reshetnikova, L., Clark, B.F.C., and Nyborg, J. (1995). Crystal Structure of the Ternary Complex of Phe-tRNA^{Phe}, EF-Tu, and a GTP analog. Science *270*, 1464–1472.

Poole, E.S., Major, L.L., Mannering, S.A., and Tate, W.P. (1998). Translational termination in Escherichia coli: three bases following the stop codon crosslink to release factor 2 and affect the decoding efficiency of UGA-containing signals. Nucleic Acids Res. *26*, 954–960.

Seit Nebi, A., Frolova, L., Ivanova, N., Poltarous, A., and Kisselev, L. (2000). Substitutions of the glutamine residue in ubiquitous GGQ tripeptide in human eRF1 do not entirely abolish the release factor activity. Mol. Biol. *34*, 899–900.

Selmer, M., Al-Karadaghi, S., Hirokawa, G., Kaji, A., and Liljas, A. (1999). Crystal structure of Thermotoga maritima ribosome recycling factor: a tRNA mimic. Science *286*, 2349–2352.

Song, H., Mugnier, P., Das, A.K., Webb, H.M., Evans, D.R., Tuite, M.F., Hemmings, B.A., and Barford, D. (2000). The crystal structure of human eukaryotic release factor eRF1—mechanism of stop codon recognition and peptidyl-tRNA hydrolysis. Cell *100*, 311–321.

Uno, M., Ito, K., and Nakamura, Y. (1996). Functional specificity of amino acid at position 246 in the tRNA mimicry domain of bacterial release factor *2*. Biochimie *78*, 935–943.

Wilson, D.N., Guevremont, D., and Tate, W.P. (2000). The ribosomal binding and peptidyl-tRNA hydrolysis functions of Escherichia coli release factor 2 are linked through residue *246*. RNA *6*, 1704–1713.

Yusupov, M.M., Yusupova, G.Z., Baucom, A., Lieberman, K., Earnest, T.N., Cate, J.H., and Noller, H.F. (2001). Crystal structure of the ribosome at 5.5 Å resolution. Science *292*, 883–896.

Accession Numbers

The coordinates of *E. coli* RF2 have been deposited in the Protein Data Bank with the ID code 1GQE.